

Spectral dependence of single molecule fluorescence enhancement

Palash Bharadwaj and Lukas Novotny

*Institute of Optics and Department of Physics and Astronomy,
University of Rochester, Rochester, NY, 14627, USA*

novotny@optics.rochester.edu

Abstract: The fluorescence from a single molecule can be strongly enhanced near a metal nanoparticle acting as an *optical antenna*. We demonstrate the spectral tunability of this antenna effect and show that maximum enhancement is achieved when the emission frequency is *red-shifted* from the surface plasmon resonance of the particle. Our experimental results, using individual gold and silver particles excited at different laser-frequencies, are in good agreement with an analytical theory which predicts a different spectral dependence of the radiative and non-radiative decay rates.

© 2007 Optical Society of America

OCIS codes: (260.2510) Fluorescence; (260.2160) Energy transfer; (160.4236) Nanomaterials; (240.6680) Surface plasmons.

References and links

1. P. Anger, P. Bharadwaj, and L. Novotny, "Enhancement and quenching of single-molecule fluorescence," *Phys. Rev. Lett.* **96**, 113002 (2006).
2. S. Kühn, S. U. Håkanson, L. Rogobete, and V. Sandoghdar, "Enhancement of single-molecule fluorescence using a gold nanoparticle as an optical nanoantenna," *Phys. Rev. Lett.* **97**, 017402 (2006).
3. J. N. Farahani, D. W. Pohl, H.-J. Eisler, and B. Hecht, "Single quantum dot coupled to a scanning optical antenna: a tunable superemitter," *Phys. Rev. Lett.* **95**, 017402 (2005).
4. Fu Min Huang, and D. Richards, "Fluorescence enhancement and energy transfer in apertureless scanning near-field optical microscopy," *J. Opt. A : Pure Appl. Opt.* **8**, S234-S238 (2006).
5. D. W. Pohl, "Near-field optics seen as an antenna problem," in *Near-field Optics, Principles and Applications*, X. Zhu, and M. Ohtsu, eds. (World Scientific, Singapore, 2000), pp 9-21.
6. P. Mühlischlegel, H.-J. Eisler, O. J. F. Martin, B. Hecht, and D. W. Pohl, "Resonant optical antennas," *Science* **308**, 1607-1609 (2005).
7. K. B. Crozier, A. Sundaramurthy, G. S. Kino, and C. F. Quate, "Optical antennas: resonators for local field enhancement," *J. Appl. Phys.* **94**, 4632-4642 (2003).
8. P. J. Schuck, D. P. Fromm, A. Sundaramurthy, G. S. Kino, and W. E. Moerner, "Improving the mismatch between light and nanoscale objects with gold bowtie nanoantennas," *Phys. Rev. Lett.* **94**, 017402 (2005).
9. T. Kalkbrenner, U. Håkanson, A. Schädle, S. Burger, C. Henkel, and V. Sandoghdar, "Optical microscopy via spectral modifications of a nanoantenna," *Phys. Rev. Lett.* **95**, 200801 (2005).
10. L. Novotny and B. Hecht, *Principles of Nano-Optics* (Cambridge University Press, Cambridge, 2006).
11. M. L. Brongersma and P. G. Kik, eds., *Surface Plasmon Nanophotonics* (Springer Series in Optical Sciences, New York, 2006).
12. Y. Xu, R. K. Lee, and A. Yariv, "Finite-difference time-domain analysis of spontaneous emission in a microdisk cavity," *Phys. Rev. A* **61**, 033808 (2000).
13. G. W. Ford, and W. H. Weber, "Electromagnetic interactions of molecules with metal surfaces," *Phys. Rep.* **113**, 195-287 (1984).
14. H. Metiu, "Surface Enhanced Spectroscopy," *Prog. Surf. Sci.* **17**, 153-320 (1984).
15. V. V. Klimov, M. Ducloy, and V. S. Letokhov, "Spontaneous emission in the presence of nanobodies," *Quantum Electron.* **31**, 569-586 (2001).

16. R. Carminati, J.-J. Greffet, C. Henkel, and J. M. Vigoureux, "Radiative and non-radiative decay of a single molecule close to a metallic nanoparticle," *Opt. Commun.* **261**, 368-375 (2006).
 17. Y. Chen, K. Munechika, and D. S. Ginger, "Dependence of fluorescence intensity on the spectral overlap between fluorophores and plasmon resonant single silver nanoparticles," *Nano Letters* **7**, 690-696 (2007).
 18. R. Carminati, M. Nieto-Vesperinas, and J.-J. Greffet, "Reciprocity of evanescent electromagnetic waves," *J. Opt. Soc. Am. A* **15**, 706-712 (1998).
 19. K. T. Shimizu, W. K. Woo, B. R. Fisher, H. J. Eisler, and M. G. Bawendi, "Surface-enhanced emission from single semiconductor nanocrystals," *Phys. Rev. Lett.* **89**, 117401 (2002).
 20. J. Azoulay, A. Debarre, A. Richard, and P. Tchenio, "Quenching and enhancement of single-molecule fluorescence under metallic and dielectric tips," *Europhys. Lett.* **51**, 374-380 (2000).
 21. V. Giannini, J. A. Sánchez-Gil, J. V. García-Ramos, and E. R. Méndez, "Electromagnetic model and calculations of the surface-enhanced Raman-shifted emission from Langmuir-Blodgett films on metal nanostructures," *J. Chem. Phys.* **127**, 044702 (2007).
 22. P. B. Johnson, and R. W. Christy, "Optical constants of the noble metals," *Phys. Rev. B* **6**, 4370-4379 (1972).
 23. L. Novotny, M. R. Beversluis, K. S. Youngworth, and T. G. Brown, "Longitudinal field modes probed by single molecules," *Phys. Rev. Lett.* **86**, 5251-5254 (2001).
 24. M. A. Lieb, J. Zavislan, and L. Novotny, "Single-molecule orientations determined by direct emission pattern imaging," *J. Opt. Soc. Am. B* **21**, 1210-1215 (2004).
-

1. Introduction

The fluorescence from a single molecule can be enhanced by a local probe acting as an optical antenna [1, 2, 3, 4], a device that efficiently converts the energy associated with free-propagating radiation to localized energy, and *vice versa*. The study of optical antennas has been undertaken only recently [5, 6, 7, 8, 9] and draws its inspiration from near-field optics [10] and nanoplasmonics [11]. In future technology, optical antennas are likely to be employed for improving the efficiency of photovoltaics, light emitting devices and biosensors. An excited molecule placed near an optical antenna can be viewed as a transmitter and, similarly, a molecule in its ground state and getting excited by the localized field near the optical antenna acts as a receiver. Hence, an antenna used to enhance the fluorescence from a single molecule acts as a two-way antenna [1]. In this article we investigate both experimentally and theoretically the spectral dependence of single molecule fluorescence enhancement near an optical antenna made of a simple gold or silver particle attached to a pointed glass tip. Although a spherical particle is not the most efficient antenna it has a simple geometry that makes a quantitative comparison between theory and experiment possible. The findings of our study can be readily extended to other antenna geometries.

The challenge associated with the design of optical antennas is the fact that a simple down-scaling of well-established radiowave and microwave antennas into the optical frequency regime is not possible. Traditional radiowave or microwave antennas operate at frequencies much smaller than the plasma frequency ω_p of the electrons in the metal. Consequently, the conduction electrons respond 'instantaneously' to an external electric field. On the other hand, optical frequencies are near ω_p and hence the response becomes strongly material and frequency dependent. As a consequence, while the crucial parameters of a microstrip antenna (e.g. antenna gain or radiation efficiency) operating at 1 GHz depend only on its geometry and not on the particular properties of its metal components, the properties of an *optical* antenna are strongly influenced by the material-specific plasmon resonances. Not surprisingly, therefore, antennas of the same geometry but made from different metals are expected to exhibit potentially very different behavior at optical frequencies. As optical antennas increasingly find use as probes for nanoscale optical spectroscopy, it becomes necessary to characterize and optimize them with respect to specific applications. The use of fluorescence to study optical antennas allows a quantitative understanding of the loss mechanisms that are present in real materials at optical wavelengths. In this article, we investigate the effect of a metal nanoparticle antenna on the fluorescence rate of a nearby single fluorophore, and demonstrate that material properties

and the excitation wavelength are key parameters in determining the maximal enhancement of fluorescence caused by the antenna.

As shown in Fig. 1, we use a simple antenna geometry in the form of a spherical metal (gold or silver) nanoparticle attached to a glass tip. This choice makes the theoretical modeling of the system less challenging and the experimental fabrication of the antennas reproducible. In the next section, we theoretically analyze the fluorescence rate of a molecule placed near a metal nanoparticle. In particular, we present approximate analytical solutions that elucidate the role of the particle's surface plasmon resonances on the radiative and non-radiative decay rates of the molecule. In section 3 we present our experimental results and compare the results with theory.

2. Theory

The fluorescence rate γ_{em} of a single molecule can be expressed as the product of excitation rate γ_{exc} and quantum yield q , defined as the fraction of radiative transitions from excited to ground state to the total decay rate. Treating the excitation and emission processes independently is legitimate because there is no coherence between the two processes. The fluorescence enhancement can then be expressed as

$$\frac{\gamma_{em}}{\gamma_{em}^o} = \frac{\gamma_{exc}}{\gamma_{exc}^o} \frac{q}{q^o}, \quad (1)$$

where the superscript 'o' indicates the corresponding free-space quantity. Below saturation, the excitation rate γ_{exc} is proportional to $|\mathbf{E} \cdot \mathbf{p}|^2$, with \mathbf{E} being the local electric field and \mathbf{p} the transition dipole moment. On the other hand, within the validity of Fermi's Golden Rule, the decay rate of the excited molecule is expressed by the weighted sum of possible decay channels. The latter corresponds to the electromagnetic density of states defined by the Green's function of the system that is embedding the molecule. Because the Green's function is the response of a

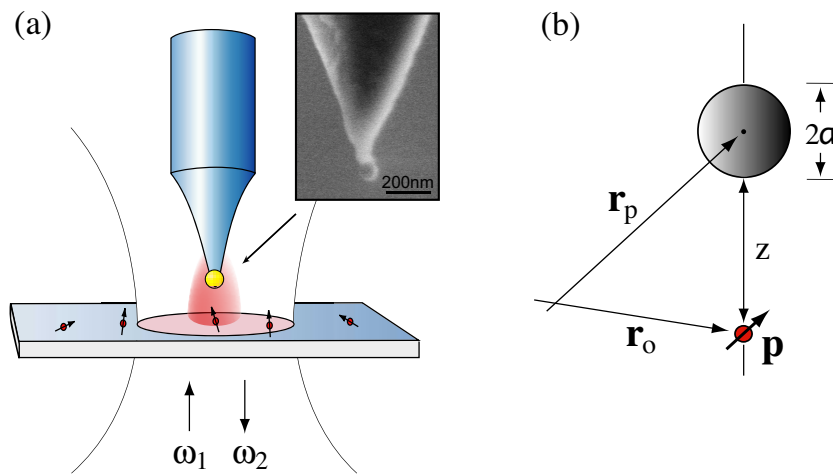


Fig. 1. (a) Schematic of the experiment. An optical antenna in the form of a gold or silver nanoparticle attached to the end of a pointed glass tip is interacting with individual fluorescent molecules excited at frequency ω_1 and emitting at frequency ω_2 . The inset shows an SEM image of a 80nm gold particle attached to an HF etched glass tip. (b) Definition of coordinates used in the theoretical analysis.

point source (dipole) it is possible to represent the emitting molecule by a classical dipole [12, 10]. Let us denote the decay rate of the excited molecule in *absence* of the optical antenna as $\gamma^o = \gamma_r^o + \gamma_{nr}^o$, where γ_r^o and γ_{nr}^o are the radiative and nonradiative decay rates of the excited molecule, respectively. Notice that γ_{nr}^o accounts for nonradiative losses *inside* the molecule only, i.e. it is an intrinsic property independent of antenna-molecule distance. The intrinsic quantum yield of the isolated molecule is defined as $q^o = \gamma_r^o / (\gamma_r^o + \gamma_{nr}^o)$. The presence of the particle antenna, however, introduces an additional nonradiative rate γ_{abs} , thereby modifying the quantum yield to $q = \gamma_r / (\gamma_r + \gamma_{nr} + \gamma_{abs})$. Using the definition of q^o , this can be recast as

$$q = \frac{\gamma_r / \gamma_r^o}{\gamma_r / \gamma_r^o + \gamma_{abs} / \gamma_r^o + (1 - q^o) / q^o}. \quad (2)$$

Here, γ_r is the radiative rate in presence of the optical antenna. We assumed that the antenna does not influence the intrinsic nonradiative rate, i.e. $\gamma_{nr} = \gamma_{nr}^o$. For large separations between molecule and particle we have $\gamma_{abs} \rightarrow 0$ and $\gamma_r \rightarrow \gamma_r^o$, and hence $q = q^o$. On the other hand, for a molecule with high intrinsic quantum yield ($q^o = 1$) we obtain $q = \gamma_r / (\gamma_r + \gamma_{abs})$ and hence γ_{abs} is the only nonradiative decay channel. Using the multiple multipole (MMP) method [10] we have calculated the different decay rates and the quantum yield for different particle-molecule configurations and for different particle materials following a theory outlined previously [1]. The results will be presented and discussed in the following. However, in order to establish an intuitive understanding we first introduce an approximate analysis which agrees surprisingly well with the rigorous calculations.

Let us first analyze the energy transfer rate to the particle (γ_{abs}). This rate can be deduced from the power P_{abs} that is radiated by the molecule and absorbed in the particle. Once P_{abs} is known, the normalized energy transfer rate is calculated as $\gamma_{abs} / \gamma_r^o = P_{abs} / P_o$, with $P_o = |\mathbf{p}|^2 \omega_2^2 k_2^3 / (12\pi\epsilon_o)$ being the power radiated by a classical dipole with frequency ω_2 and dipole moment \mathbf{p} , and the associated wavevector being defined as $k_2 = \omega_2 / c$. For very small distances between molecule and particle the curvature of the particle's surface can be neglected and the environment 'as seen' by the molecule is a plane interface. Using electrostatic image theory [10] the power emitted by the molecule and absorbed inside a half-space with frequency-dependent dielectric constant $\epsilon(\omega_2)$ can be calculated and the energy transfer rate becomes

$$\frac{\gamma_{abs}}{\gamma_r^o} = \frac{3}{16} \text{Im} \frac{\epsilon(\omega_2) - 1}{\epsilon(\omega_2) + 1} \frac{1}{k_2^3 z^3} \frac{(p_x^2 + p_y^2 + 2p_z^2)}{|\mathbf{p}|^2}, \quad (3)$$

where z is the molecule-surface separation and $\mathbf{p} = [p_x, p_y, p_z]$. Equation 3 was derived by integrating the dissipated power density $(\omega_2 \epsilon_o / 2) \text{Im}\{\epsilon\} \mathbf{E} \cdot \mathbf{E}^*$, \mathbf{E} being the electrostatic dipole field, over the volume of the half-space. Higher-order correction terms to this expression can be derived as outlined in the literature [13, 14, 15].

The derivation of the radiative decay rate γ_r makes use of the fact that the scattered power P_r from a particle much smaller than the wavelength of light originates mostly from the particle's induced dipole. Higher-order multipole terms give rise to dissipation. Using $\gamma_r / \gamma_r^o = P_r / P_o$, the normalized power radiated by the system of molecule and particle is calculated as

$$\frac{\gamma_r}{\gamma_r^o} = \frac{|\mathbf{p} + \mathbf{p}_{induced}|^2}{|\mathbf{p}|^2} = \left| \mathbf{n}_p + k_2^2 \frac{1}{\epsilon_o} \vec{\alpha}_p(\omega_2) \vec{\mathbf{G}}(\mathbf{r}_p, \mathbf{r}_o; \omega_2) \mathbf{n}_p \right|^2, \quad (4)$$

where $\vec{\alpha}$ is the particle's polarizability, $\vec{\mathbf{G}}$ is the free-space Green's dyadic, \mathbf{n}_p is the unit vector in direction of the molecule's dipole moment, and \mathbf{r}_o and \mathbf{r}_p are the position vectors of molecule and particle, respectively. Equations 2-4 define the quantum yield q of the molecule placed next to a particle characterized by dielectric constant ϵ and polarizability $\vec{\alpha}$. Our theory predicts that

γ_r depends on the shape and material of the particle (ϵ and $\vec{\alpha}$) whereas γ_{abs} depends only on the material properties (ϵ).

For a spherical particle, the quasi-static polarizability is calculated as [10]

$$\vec{\alpha}(\omega_2) = 4\pi\epsilon_o a^3 \frac{\epsilon(\omega_2) - 1}{\epsilon(\omega_2) + 2} \vec{\mathbf{I}}, \quad (5)$$

where a is the particle radius and $\vec{\mathbf{I}}$ the unit dyad. The polarizability in Eq. 5 can be extended to include radiation reaction [16] but the contribution of this additional term is marginal. Evaluation of Eq. 4 in the non-retarded (near-field) limit leads to

$$\frac{\gamma_r}{\gamma_r^o} = \left| 1 + 2 \frac{a^3}{(a+z)^3} \frac{\epsilon(\omega_2) - 1}{\epsilon(\omega_2) + 2} \right|^2, \quad (6)$$

where, for simplicity, we assumed a molecule orientation such that $p_x = p_y = 0$. The enhancement of the radiative rate is at a maximum at $z = 0$. It amounts to $|3\epsilon/(\epsilon + 2)|^2$ for a vertically aligned molecule ($p_x = p_y = 0$) and to $|3/(\epsilon + 2)|^2$ for a horizontally aligned molecule ($p_z = 0$). On the other hand, according to Eq. 3 the energy transfer rate at $z = 0$ goes to infinity and hence the quantum yield drops to zero. For small distances z , the radiative rate enhancement in the denominator of Eq. 2 can be ignored and the quantum yield becomes a simple function of distance and material. It is important to notice that γ_{abs} has a maximum at the frequency determined by $\epsilon(\omega_2) + 1 = 0$, whereas the maximum of γ_r occurs at $\epsilon(\omega_2) + 2 = 0$. For a spherical metal particle characterized by a free-electron gas (Drude model) the shape-dependent plasmon resonance given by $\epsilon(\omega_2) + 2 = 0$ is *red-shifted* from the dissipative resonance of $\epsilon(\omega_2) + 1 = 0$. It is not surprising, therefore, that maximum fluorescence enhancement occurs when the molecule emits even to the *red* of the plasmon resonance of the particle, rather than at it [17].

Let us now turn to the excitation rate γ_{exc} which is determined by both the incident laser field \mathbf{E}_o and the secondary field \mathbf{E}_s , i.e. the enhanced field by the particle. For weak excitation (below saturation) we have $\gamma_{exc} \propto |\mathbf{p} \cdot [\mathbf{E}_o(\mathbf{r}_o, \omega_1) + \mathbf{E}_s(\mathbf{r}_o, \omega_1)]|^2$, where ω_1 is the excitation frequency. We assume that the particle is small compared with the wavelength and that it can be represented by a polarizability $\vec{\alpha}(\omega_1)$. In this case, the secondary field can be expressed in terms of the Green's function as $\mathbf{E}_s(\mathbf{r}_o) = (k_1^2/\epsilon_o) \vec{\mathbf{G}}(\mathbf{r}_o, \mathbf{r}_p; \omega_1) \vec{\alpha}(\omega_1) \mathbf{E}_o(\mathbf{r}_p)$ and the enhancement of the excitation rate becomes

$$\frac{\gamma_{exc}}{\gamma_{exc}^o} = \frac{|\mathbf{n}_p \cdot [\vec{\mathbf{I}} + k_1^2 \vec{\mathbf{G}}(\mathbf{r}_o, \mathbf{r}_p; \omega_1) \vec{\alpha}(\omega_1)/\epsilon_o] \mathbf{n}_{E_o}|^2}{|\mathbf{n}_p \cdot \mathbf{n}_{E_o}|^2}. \quad (7)$$

where \mathbf{n}_{E_o} is the unit vector in direction of \mathbf{E}_o . We used $\mathbf{E}_o(\mathbf{r}_p) = \mathbf{E}_o(\mathbf{r}_o)$ because $|\mathbf{r}_p - \mathbf{r}_o| \ll \lambda$. For a spherical particle with polarizability α defined in Eq. 5 we obtain

$$\frac{\gamma_{exc}}{\gamma_{exc}^o} = \left| 1 + 2 \frac{a^3}{(a+z)^3} \frac{\epsilon(\omega_2) - 1}{\epsilon(\omega_2) + 2} \right|^2. \quad (8)$$

As before, we retained only the near-field terms in $\vec{\mathbf{G}}$ and assumed $p_x = p_y = 0$. It turns out that the expressions for $\gamma_{exc}/\gamma_{exc}^o$ [Eq. 8] and γ_r/γ_r^o [Eq. 6] are identical, a property that is ascribed to reciprocity [3, 18, 19, 20, 21]. However, Eqs. 8 and 6 appear identical because the dipole orientation was restricted to point along a Cartesian axis. For arbitrary dipole orientations the two expressions are not identical because different dipole components interfere in Eq. 8 whereas in Eq. 6 they do not!

In order to estimate the validity of the approximations derived for the different rates we have compared the approximations with rigorous calculations based on the MMP method. Figure 2 shows the results for a molecule with $q^o = 1$ placed next to a 60 nm gold particle irradiated with light of wavelength at $\lambda = 650$ nm. For simplicity, we assumed $\omega_1 \approx \omega_2$. The dielectric constant is inferred from interpolated experimental data [22]. The dashed curves derived with the approximate formulas overlap nearly perfectly with the solid curves derived with the MMP method. This remarkable agreement validates the finding that fluorescence quenching (γ_{abs}) is largely independent of the particle geometry. Fluorescence quenching becomes important at small distances between molecule and particle surface and for such small distances the particle surface is well approximated by a plane boundary. Thus, the only degrees of freedom for minimizing γ_{abs} are the choice of material and the excitation frequency. On the other hand, besides a different spectral dependence, the radiative decay rate and the excitation rate are strongly dependent on the geometry of the particle and hence can be optimized by suitable optical antenna design. For larger particles we have found that the approximation becomes less accurate, mainly because of the insufficiency of retaining only the near-field terms in the Green's function. Furthermore, the scattering efficiency of large particles becomes dependent on higher order multipoles and hence the representation by a simple polarizability is no longer sufficient.

Using the approximate theory outlined above, we have carried out a spectral analysis of the fluorescence enhancement for both silver and gold nanoparticles. As before, we assume $p_x = p_y = 0$ and $q^o \approx 1$. Figure 3(a) shows that the enhancement is strongly wavelength dependent. At $\lambda = 650$ nm the enhancements for silver and gold particles differ only slightly whereas for bluer wavelengths, e.g. at $\lambda = 488$ nm, the enhancement for silver particles is predicted to be much stronger than the enhancement for gold particles. Figure 3(a) demonstrates that the

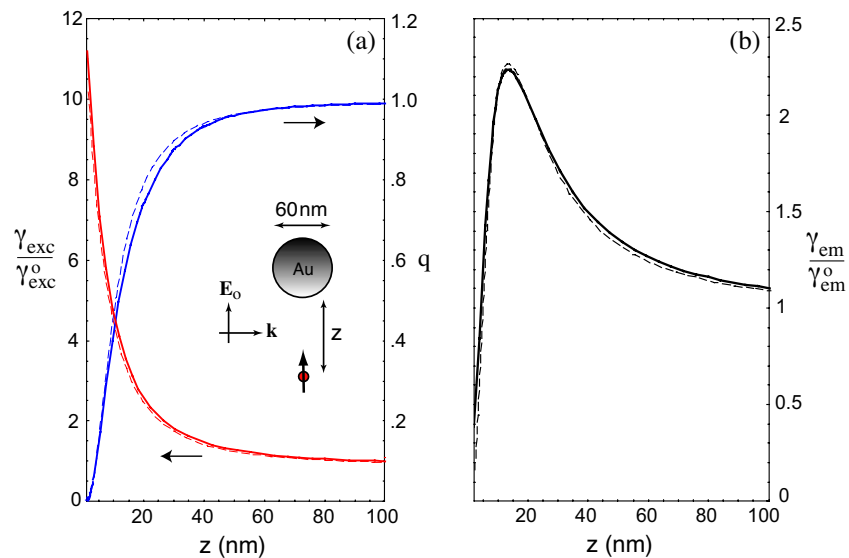


Fig. 2. Fluorescence enhancement near a 60 nm gold nanoparticle excited with wavelength $\lambda = 650$ nm. (a) Quantum yield (blue) and excitation rate enhancement (red). (b) Emission enhancement. The emission wavelength is taken to be same as the excitation wavelength. The solid curves are exact results based on the MMP method and the dashed curves are approximations (Eqs. 3, 6, 8).

maximum fluorescence enhancement is obtained for wavelengths *red-detuned* from the surface plasmon resonance. Figure 3(b) shows the calculated distance dependence of the fluorescence enhancement for an excitation and emission wavelength of $\lambda = 488\text{nm}$. Because this wavelength is blue-shifted from the plasmon resonance of a gold particle we expect no significant enhancement and this is indeed reflected by the curve for the gold particle.

3. Experiments

We have experimentally tested the predictions shown in Fig. 3 using two different excitation wavelengths (488 nm and 637 nm) and two different molecules (Alexa488 and Nile Blue). Single molecule samples were prepared by spincoating the molecules on a glass coverslip and then again spincoating a thin layer ($< 5\text{ nm}$) of polymer (PMMA) on top. The antenna, in this case an 80 nm gold or silver particle, is raster-scanned over the polymer surface at variable heights. The theoretical curves shown in Fig. 3 do not account for the presence of a dielectric interface. As shown previously [1], the dielectric interface increases the fluorescence enhancement by a factor 2 – 3 which has to be taken into account when comparing the here derived theory with the experimental results presented in the following.

The molecules are excited by a standard confocal arrangement with a radially polarized excitation laser beam and a single-photon counting detector (c.f. Fig. 1(a)). The particle (antenna) can be positioned into the focus using a shear-force feedback mechanism. We can either generate a fluorescence rate image by raster-scanning the particle at a controllable but constant distance (typically $\sim 5\text{ nm}$) over the sample surface, or we can position the particle over a selected molecule and record the fluorescence rate as a function of the particle-sample distance. The results of our experiments at using $\lambda = 488\text{ nm}$ excitation are summarized in Fig. 4 which

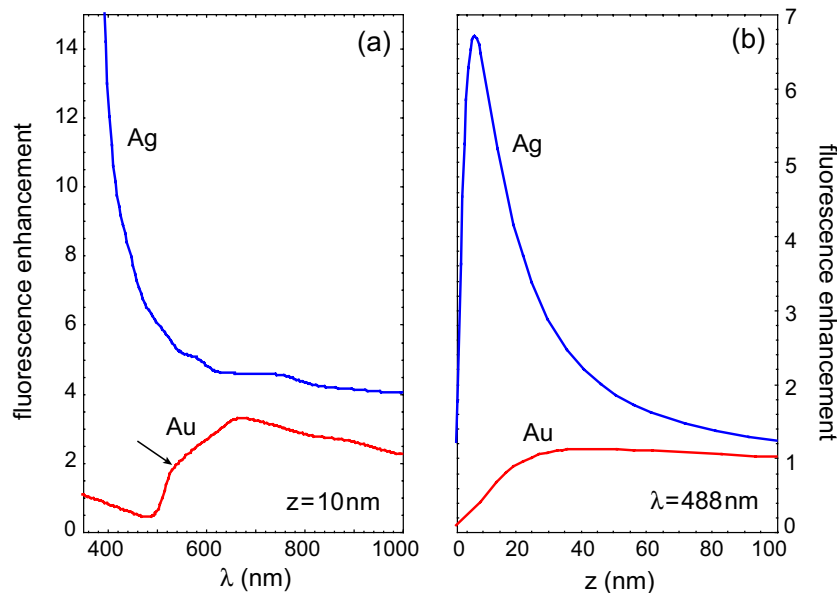


Fig. 3. Calculated fluorescence enhancement near gold and silver nanoparticles of 80 nm diameter. (a) Spectral dependence at a distance of $z = 10\text{ nm}$. The arrow marks the plasmon resonance of a gold nanoparticle in air. The corresponding resonance for silver is at around 360 nm. (b) Distance dependence at a wavelength of $\lambda = 488\text{ nm}$. Experimental data from Ref. [22] was used for the dielectric constants of gold and silver.

shows fluorescence rate images recorded with both a gold particle (left) and a silver particle (right). In order to obtain roughly equal fluorescence intensities ($\sim 10\text{kHz}$), the excitation power in Fig. 4(a) had to be increased by roughly ten times over the power used in Fig. 4(b). For the gold particle, the near-field enhancement is barely discernible whereas for the silver particle the near-field enhancement is so strong that the far-field fluorescence background is at the level of the detector's dark counts. A comparison of the two images in Fig. 4 qualitatively validates the theoretical predictions displayed in Fig. 3. However, to be more quantitative we recorded the distance dependence of the fluorescence enhancement for both gold and silver particles.

After identifying the orientations of various single molecules embedded in the polymer matrix from either confocal or near-field emission patterns [23, 24] we selected a vertically oriented molecule ($p_x \approx p_y \approx 0$) and positioned it into the laser focus and underneath the gold or silver particle. The fluorescence rate was then recorded as a function of the vertical position of the particle. In order to observe quenching at short distances the thickness of the PMMA layer was chosen to be sufficiently thin. Figure 5 shows recorded approach curves for two different combinations of particles and laser wavelengths. In Fig. 5(a) we used a silver particle to enhance the fluorescence of an Alexa488 molecule excited with a laser wavelength of $\lambda = 488\text{nm}$, and in Fig. 5(b) a gold particle was used in combination with a Nile Blue molecule and a wavelength of 637nm . The silver particle gives an enhancement of a factor of 13 – 15 whereas the gold particle enhances the fluorescence about 8 – 9 fold. The ratio between these enhancements is consistent with the theoretical predictions of Fig. 3(a). Both approach curves shown in Fig. 5 clearly show that the fluorescence enhancement starts to drop for very short distances, indicative for the onset of quenching. Theory predicts that fluorescence should drop to zero when the molecule is in direct contact with the particle but this cannot be verified experimentally because of the finite thickness of the PMMA layer that is used to immobilize and orient the dye molecules.

In conclusion, we have presented a simple analytical model for calculating the fluorescence rate of a single molecule close to a nanoparticle antenna. The model highlights the role of an-

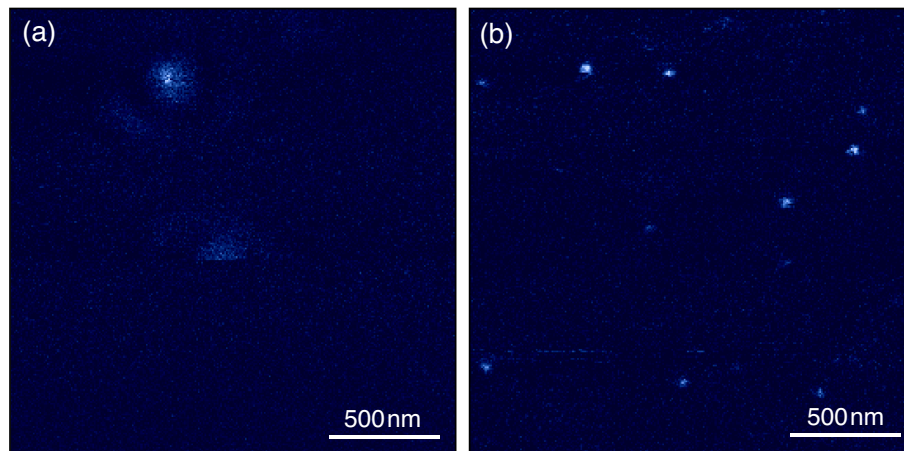


Fig. 4. Near-field fluorescence rate images of Alexa488 molecules recorded using (a) an 80 nm gold particle and (b) an 80 nm silver particle excited at $\lambda = 488\text{nm}$. At this wavelength the enhancement for the silver particle is more than 10 times stronger than for the gold particle, consistent with the predictions of Fig. 3. The image in (a) reflects the confocal excitation spot whereas the image in (b) represents the localized fields at the silver particle.

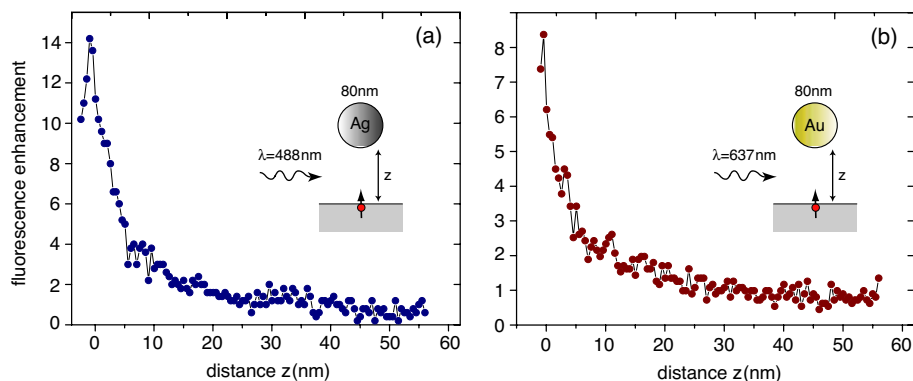


Fig. 5. Fluorescence enhancement as a function of molecule-particle separation for two different particles (gold and silver) and two different excitation wavelengths. (a) Alexa488 molecule excited by a 80nm silver particle irradiated with $\lambda = 488$ nm. (b) Nile Blue molecule excited by a 80nm gold particle irradiated with $\lambda = 637$ nm. The unity baseline for fluorescence enhancement is determined using the measured fluorescence when the antenna is retracted far away from the molecule (~ 500 nm). Both curves show a decrease at short distances due to fluorescence quenching.

tenna plasmon resonances in determining the relative strength of various rates involved in the fluorescence process, and its predictions are in good agreement with more rigorous MMP calculations. Our single molecule experiments validate the theory and demonstrate that nanoplasmonic enhancement of single molecule fluorescence is strongly frequency dependent. For molecules emitting to the blue of the surface plasmon resonance the fluorescence can be quenched whereas for molecules emitting to the red of the surface plasmon resonance the fluorescence can be strongly enhanced. We believe these findings are general and not only specific to spherical particles, and that they provide intuitive guidelines for efficient optical antenna design. Future work will concentrate on the development of optical antennas providing increased enhancement, stronger field localization, and tunable spectral properties.

Acknowledgments

This research was funded by the National Institutes of Health through grant EB004588 and the U.S. Department of Energy through grant DE-FG02-01ER15204. We are grateful to Shanlin Pan and Lewis Rothberg for help with surface chemistry and to Pascal Anger for initial experiments and fruitful discussions.